Astron. Astrophys. 318, 416–428 (1997)

ASTRONOMY
AND
ASTROPHYSICS

Rotation of the outer disc from classical cepheids⋆

F. Pont, D. Queloz, P. Bratschi, and M. Mayor

Geneva Observatory, CH-1290 Sauverny, Switzerland

Received 19 April 1996 / Accepted 13 June 1996

Abstract. Radial velocities and distances have been measured for a sample of 48 remote classical cepheids located in the outer disc of the Galaxy ($118^0 < l < 274^0$). The distances are determined from BVI photometry, with semi-empirical metallicity corrections calibrated on the Magellanic Clouds. Using these cepheids as tracers, the rotation curve of the disc is determined between R_0 and $2R_0$. The result is a flat rotation curve about 30 km s^{-1} lower than θ_0, V_{rot} = 193±4 km s^{-1} for R_0 = 8.5 kpc and θ_0 = 220 km s^{-1} assumed, or V_{rot} = 167 ± 4 km s^{-1} for R_0 = 8 kpc and θ_0 = 200 km s^{-1}.
The possible presence of non-axisymmetric components in the rotation of the outer disc is considered. We find a very small or vanishing value for any radial motion of the LSR or expansion/contraction motion. In particular, the data exclude large radial motions such as have been proposed in some models to account for features observed in the kinematics of the gas.
The rotation curve indicated by cepheids is markedly lower than that currently derived using HII regions. Possible explanations are examined. A real kinematical difference is possible, caused for instance by radial motions in the gas induced by spiral arms, but an important distance scale difference is not excluded. A systematic error added to a high dispersion on HII region distances could explain the mismatch.

Key words: stars: distance – kinematics – cepheids – Galaxy: kinematics and dynamics

1. Introduction

It is now well established that the rotation curves of spiral galaxies, including the Milky Way, are not decreasing at large radii, but generally remain nearly flat even beyond the end of the optical disc, revealing the presence of dark matter.

The rotation curve of the Milky Way itself has proved hard to determine, especially for $R > R_0$, because of our unfavorable position in the middle of its disc. As the tangent-point method using HI gas cannot be applied towards the outer disc, one needs a population of tracers - preferably bright – whose radial velocity and distance can be determined independently. Recent determinations using planetary nebulae, clusters or HII regions include Schneider & Terzian (1983), Hron (1987), Fich et al. (1989). For a different approach using HI, see Merrifield (1992).

These studies outline a rotation curve with a dip beyond the solar radius, then flat or rising at large radii. The most widely cited method consists of measuring the radial velocity of the gas in HII regions and their distance by ZAMS fitting to the exciting stars (see review in Fich & Tremaine 1991). This seems to indicate a rotation curve that rises to 250 km s^{-1} from R=10 kpc outwards (for R_0 = 8.5 kpc and θ_0 = 220 km s^{-1} assumed). But the data are sparse and scattered beyond R=12kpc and these values are not unambiguously defined. Moreover the distance determination for HII regions is a very delicate procedure (Turbide & Moffat 1993).

Hence the idea of extending a precise determination of the rotation curve to the outer disc using classical cepheids is a reasonable alternative. Their intrinsic brightness, reliability as distance indicators and young age make classical cepheids ideal tracers for studying the rotation curve of the Milky Way (Joy 1939, Stibbs 1956). Recent studies using cepheids define the rotation curve in the range R=6–11 kpc (Caldwell & Coulson 1987, Pont et al. 1994). Beyond this range, the objects become fainter (Fig. 1), and before this study very few had been measured in radial velocity.

This paper presents the results of a programme aimed at extending the determination of the rotation curve out to $R \simeq 2\,R_0$ using cepheids. Our strategy has been to choose cepheids beyond $R \simeq 11$ kpc along the two directions $l \sim 135^o$ and $l \sim 225^o$. To this was added a control sample in the anticentre direction ($l \sim 180^o$) in order to detect a possible non-axisymmetric component in the velocity field – towards the anticentre, the line of sight is perpendicular to the rotation velocity, and only non-axisymmetric motions affect the radial velocity. The gradual recognition of the fact that the Galaxy probably contains a bar or triaxial spheroid (Blitz & Spergel 1991, Weinberg 1992, Dwek et al. 1995), as well as the asymmetries observed in HI kinematics, have recently led to some non-axisymmetric models for the Galaxy (Blitz & Spergel 1991, Kuijken 1994,

Send offprint requests to: F. Pont

⋆ Based on observations made at the Observatoire de Haute-Provence, France and at the European Southern Observatory, La Silla, Chile.

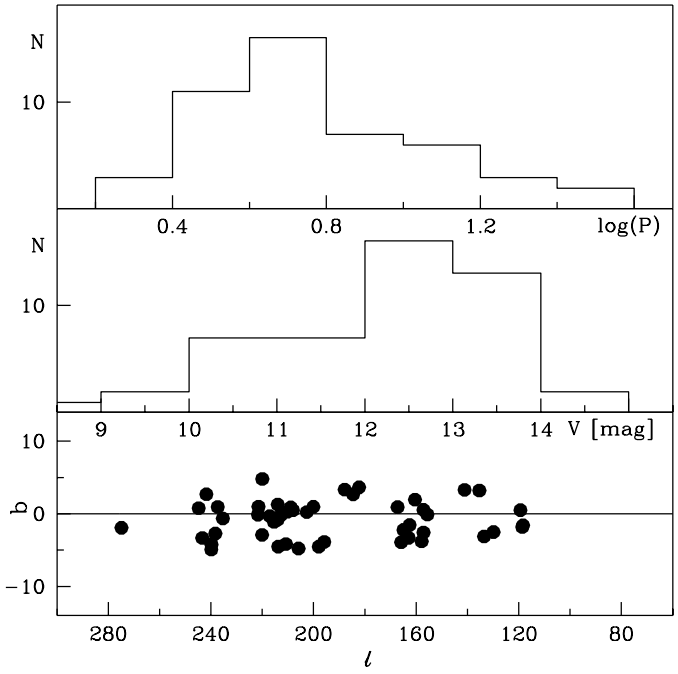

Fig. 1. General characteristics of the sample: distribution of periods (top), magnitudes (middle) and galactic coordinates (bottom)

Kuijken & Tremaine 1994). These models make testable predictions about the velocity field of the outer disc.

The target stars have been selected as the classical cepheids (DCEP) and cepheids of unknown type (CEP) in the GCVS (Kholopov 1985) which were estimated, based on photometric data found in the stellar database SIMBAD, to be situated beyond R=11 kpc by a crude distance estimate.

The resulting list contains 48 objects, of V magnitudes between 9 and 15, periods between 2 and 26 days, 11 in the north ($l < 160^o$), 11 towards the anticentre ($160^o < l < 200^o$) and 26 in the south ($200^o < l$). This uneven distribution reflects the fact that the absorption is much lower in the third galactic quadrant. We have measured these objects in radial velocity, and in photometry when the data available were not sufficient to obtain reliable distances.

The distributions of visual magnitudes, periods and galactic coordinates for the sample are displayed in Fig. 1.

Sect. 2 of this article presents the radial velocity and photometric data. Distances are computed in Sect. 3, using period-luminosity relations corrected for metallicity effects. Sect. 4 presents the resulting rotation curve, and examines the non-axisymmetric component of the velocity field. In Sect. 5, the results are compared with other observational studies and confronted to some models, and the effects of modifying some assumptions are examined.

2. Observations

The observations began in September 1993 during a test run on the newly-built spectrometer "ELODIE ", and were carried out during 12 different observing runs at the Observatoire de Haute-Provence (OHP, France), Pic du Midi (France) and La Silla (Chile) between September 1993 and January 1995.

2.1. Radial velocities

Radial velocities have been collected at OHP, with the spectrometer ELODIE (Baranne et al. 1996) installed on the 1.93-m telescope, for the faintest half of the sample, and with the CORAVEL spectrometer (Baranne et al. 1979) on the 1-m Swiss telescope at OHP for the brightest half. A few measurements were also made with the southern CORAVEL on the Danish 1.5-m telescope at ESO (Chile).

ELODIE is a high-resolution echelle spectrometer. Radial velocities are calculated from the spectra with an on-line reduction procedure using numerical correlation with a binary mask imitating a F0 dwarf. With this method reliable velocities can be obtained from spectra with a signal-to-noise ratio as low as 2. Typical exposure times were from 20 to 45 minutes. ELODIE can reach an accuracy of 15 m s^{-1} or better on bright objects, with frequent calibration, but since such accuracy is not necessary for our programme, we have decided to use a mean calibration of the spectrograph zero-point to speed up the observations. This increases the average instrumental uncertainty by about 100-200 m s^{-1}. By adding the photon noise we then have a typical radial velocity uncertainty of 300-400 m s^{-1}.

The mean uncertainty of the CORAVEL set of measurements is 0.55 km s^{-1}.

157 radial velocity measurements were made with ELODIE, and 174 with CORAVEL . The average number of measurements per object is between 7 and 8, and a particular care has been taken to sample regularly the whole pulsation cycle. For galactic kinematics, only the centre-of-mass velocity (γ velocity) is needed, and in most cases 5 well-spaced measurements are sufficient to determine the γ velocity with a sufficient accuracy ($\sigma = 2 - 3$ km s^{-1}, see Pont et al. 1994).

The measurements are available in electronic form (ftp 130.79.128.5 or http:://cdsweb.u-strasbg.fr/Abstract.html). Fig. 2 displays the resulting radial velocity curves.

The cepheid CI Per, originally included in the sample, was removed because the cross-correlation function showed some unexpected characteristics that may show the star to be a spectroscopic binary. Spectra with a higher signal-to-noise ratio would be necessary to settle this question.

2.2. Photometry

Although our main effort concerned radial velocities, we also obtained photometry for most objects in the sample, since the existing data were not sufficient to compute reliable reddenings and distances. The observations were made in the southern hemisphere using the CCD on the Swiss 0.7-m telescope at ESO (Chile) in BVRI filters, with Geneva BV (Rufener & Nicolet 1988), Gunn R (Thuan & Gunn 1976) and Cousins I (Cousins 1974). The CCD and reduction procedure are described in Blecha et al. (1990). The raw flux is obtained by inte-

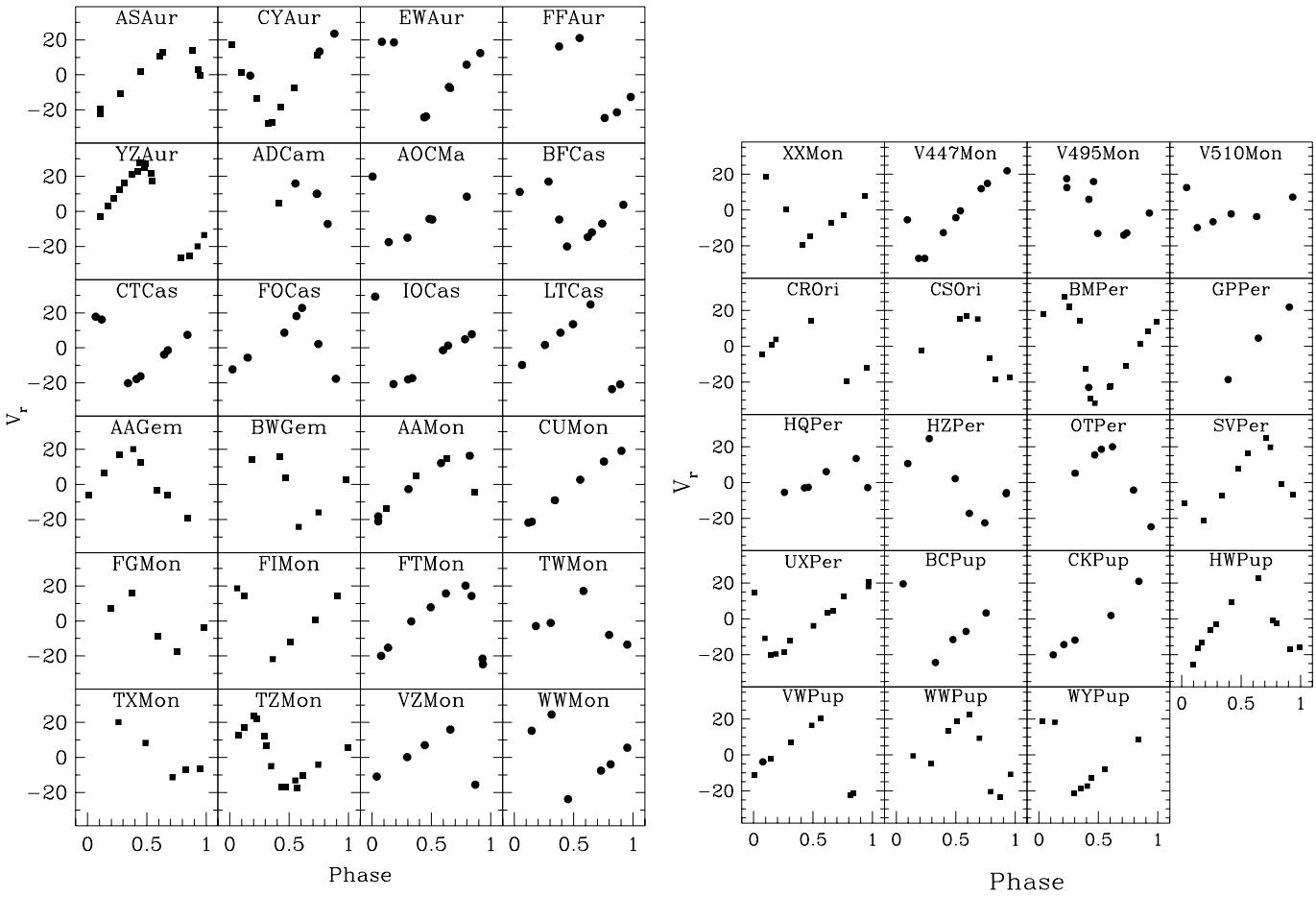

Fig. 2. Radial velocity measurements for the cepheids in our sample, as a function of phase. The velocities are reported on a single scale, relative to the γ velocity, for all objects. Circles indicate ELODIE measurements, squares CORAVEL measurements.

gration with an aperture of 40 pixels (16 arc-seconds), and the sky background determined individually for each measurement as a clipped mode of the intensity distribution on the peripheral annulus of the aperture. Extinction coefficients were calculated with a quadratic time dependence for each night using standard stars observed over a large airmass range. The method is similar to that described by Manfroid (1985). Two sets of standards were used: all-sky standards from Rufener (1988) for B and V, and equatorial standards from Menzies et al. (1991) for R and I. Linear colour equations are determined for each run (Bratschi & Blecha 1996). One CCD exposure was taken through each filter. The exposure times are adapted for each filter according to the colour of the observed star, as entered by the observer, with a target error of 1%. As the exposure time is limited by the telescope tracking system to a few minutes, the uncertainties on B for the faintest stars in the sample are higher ($\sim$3%).

Altogether, it amounts to 226 measurements for 21 stars, an average of about 11 measurements per star.

In the northern hemisphere, inclement weather and technical problems prevented us from getting any data during a one week run on the 2-m telescope at Pic du Midi (France). Most of the data come from Arne Henden at USRA/USNO Flagstaff, who very kindly agreed to add some of our objects to his measurement campaign and made available to us more than 200 BVRI (Johnson and Kron-Cousins system) measurements prior to publication.

We also used numerous measurements published by L. Berdnikov (1987, 1993, 1995).

The visual magnitude curves are shown on Fig. 3, using the data of this article and of Henden. The raw data are available in electronic form (ftp 130.79.128.5 or http:://cdsweb.u-strasbg.fr/Abstract.html).

2.3. Mean values

Mean photometric values and γ velocities are presented in Table 1 together with general data for the programme stars. Galactic coordinates and periods are taken from the GCVS and the SIMBAD database except when indicated in the notes. The periods of FT Mon, VZ Mon and V510 Mon were slightly modified. V510 Mon in particular seems to have undergone a significant period change since its photographic detection by Wachmann (1966). Mean values for magnitudes and radial velocities were calculated either by fitting a 2nd to 5th order Fourier curve on the data when the number of measurements was sufficient, or

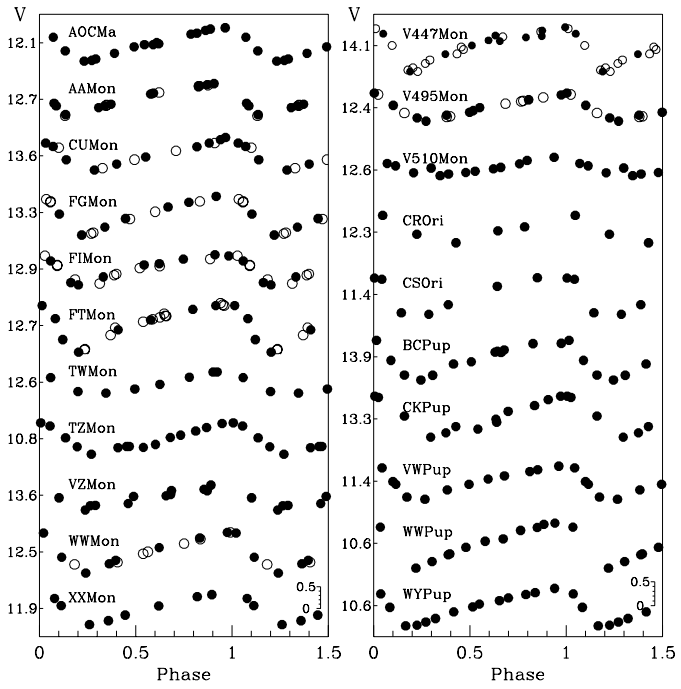

Fig. 3. Photometric measurements obtained for the cepheids in our sample. Only measurements in V are plotted, but B, R and I were also measured in most cases. The curves are shifted vertically for clarity. The vertical scale is identical for all stars and is indicated at the lower right. Filled circles: our data. Open circles: from Henden (1996, priv. comm.).

by fitting the curve of another well-measured cepheid of similar period (a method described in Pont et al. 1994) for low numbers of measurements. The number of measurements used in each fit is indicated. The Geneva B were not used since the conversion from the CCD to the photoelectric Geneva system was found to be non-linear for the faintest objects.

3. Distance determination

The distance of classical cepheids can be known with a high accuracy using period-luminosity (PL) and period-luminosity-colour (PLC) relations (see for instance the review by Feast & Walker 1987), making them a privileged standard candle. Some care must be taken in applying these relations to outer disc cepheids for two reasons: high reddening and metal deficiency. The objects in our sample have typical reddenings between 0.5 and 1 mag, and metallicities probably ranging between the LMC and SMC values (assuming a metallicity gradient in the disc of -0.05 to -0.10 dex/kpc). In order to obtain reliable distances, it is thus necessary to get precise reddenings, and to allow for metallicity effects on the PL/PLC relations. These two points are related, since if the reddening is determined from the colours of the cepheid itself -as is the case in this study- it is important to take into account the effect of metallicity on the intrinsic colours of the cepheid.

The effect of metallicity on cepheid colours and magnitudes is a complex question, still far from being satisfactorily answered. Several semi-empirical corrections have been proposed (Stothers 1988, Caldwell & Coulson 1985a, Freedman & Madore 1990, Stift 1995), but a clear consensus is yet to emerge (see remarks in Feast 1991). Purely theoretical predictions (Chiosi et al. 1993) do not reproduce quantitatively the cepheid colours observed in the Magellanic Clouds. The only point on which an agreement has been reached is the insensibility of the bolometric PL relation to metallicity.

We have decided to adopt metallicity corrections derived as much as possible from observations, taking advantage of the fact that the metallicities of the stars in our sample are bracketed between LMC and SMC metallicities, for any reasonable assumption on the metal gradient in the disc. Since many cepheids have been observed in both Clouds -which are only slightly reddened– they provide an important check on colour and magnitude variations with metal deficiency.

Two sets of relations can be used to determine the reddening and distance of a cepheid. The first ones are almost exact, being consequences of physical constraints on the pulsation: the colour-colour (CC) relation for reddenings and PLC relation for distances. The second ones are only average, as a consequence of the finite width of the instability strip: the period-colour (PC) relation for reddening and PL relation for distance. It is usual to determine reddenings with a CC relation, generally B-V vs. V-I, by fitting the observed colours on an intrinsic cepheid locus (Dean et al. 1978, Fig. 4). Now, in the case of deficient, reddened objects, the PLC and CC relations are very tricky to correct for metallicity, and the reddening determination vulnerable to uncertainties in the correction and to any change, even slight, in the assumed η (E(V-I)/E(B-V)), as the angle between the reddening vector and the intrinsic locus is small (less than 10^o for short periods, up to about 20^o for longer periods, Fig. 4). In fact the combined effects of high reddening and low metallicity make this method very fragile for short-period cepheids. For the PL relations with PC reddenings on the contrary, the metal dependence can be checked with Magellanic Clouds data, and the reddening determination is not affected by the value of η or by the amount of reddening (see Fig. 5 and Appendix). Moreover, using a PL relation with PC reddenings takes advantage of the fact that the colour term in the PLC relation is numerically similar to R (reddening to absorption ratio) and the two deviations from the ridge line tend to cancel each-other in their effect on the inferred distance (Appendix, Eq. 3).

In choosing which relation to use, one has to keep in mind that for our purpose any *systematic* bias is going to affect the resulting rotation curve –especially a bias increasing with distance. The main concern must be to avoid such a bias, even if it means accepting a slightly higher dispersion.

This has led us to use a PC relation for reddening and a PL relation for distance, rather than the usual PLC/CC pair. The Appendix shows, using order-of-magnitude calculations, why for highly reddened, metal-deficient cepheids, PL distances with PC reddenings are much more robust against systematic biases, and not more scattered, than PLC distances with CC

Table 1. General, photometric and radial velocity data for outer disc cepheids

Name		l	b	P	V	$(B-V)$	$(V-I)$	n_{mes}	source$_{phot}$	V_r	ΔV_r	n_{mes}	source$_{V_r}$	note
AS	Aur	182.3	3.7	3.175	11.94	1.04	1.20:	6|6|5	2|2|2	24.71	40.9	9	C/E	1
CY	Aur	160.5	2.0	13.849	11.85	1.62	-	-|-|-	3|3|-	-14.12	51.5	11	C	
EW	Aur	165.9	-3.9	2.595	13.51	1.12	-	-|-|-	3|3|-	-33.27	48.5	8	E	2
FF	Aur	165.0	-2.2	2.121	13.72	1.02	1.31	36|36 |7	4/2|4/2|2	-32.33	46.7	5	E	3
YZ	Aur	167.3	0.9	18.193	10.33	1.41	-	-|-|-	3|3|-	-14.81	53.73	17	C	
AD	Cam	141.2	3.3	11.253	12.56	1.63	-	-|-|-	3|3|-	-56.50	35.2	5	E/C	
BF	Cas	118.4	-1.6	3.630	12.51:	1.30:	1.59:	7|7|6	2|2|2	-61.49	39.5	8	E	
CT	Cas	119.4	0.5	3.811	12.28	1.34	-	-|-|-	7|7|-	-55.28	38.0	8	E	
FO	Cas	118.7	-1.8	6.799	14.35	1.39:	1.77	45|45|7	3/2|3/2|2	-125.85	38.9	7	E	4
IO	Cas	129.9	-2.5	5.604	13.70	1.18	1.40:	34|34|8	3/2|3/2|2	-109.18	48.7	8	E	5
LT	Cas	135.4	3.2	5.905	12.59	1.29	1.58:	33|33|6	3/2|3/2|2	-68.00	48.9	7	E	
AO	CMa	239.9	-4.9	5.816	12.08	-	1.63	16|-|16	1|-|1	80.99	44.4	6	E	
AA	Gem	184.6	2.7	11.302	9.73	1.10	1.18	-|-|-	3|3|5	18.63	42.0	8	C	
BW	Gem	187.9	3.4	2.635	12.02:	1.08:	1.32:	17|17|13	2|2|2	36.90	44.7	6	C	
AA	Mon	217.1	-0.3	3.938	12.74	1.45	1.66	19|13|18	1/2|2|1/2	66.54	41.0	8	E/C	
CU	Mon	210.8	-4.2	4.708	13.63	1.47	1.72	15|10|15	1/2|2|1/2	63.84	41.0	6	E	
EE	Mon	220.0	4.8	4.809	13.03	1.11	1.35	16|16|6	2/3|2/3|2	68.90:	-	4	C	6
FG	Mon	221.7	-0.1	4.497	13.29	1.28	1.54	15|8|15	1/2|2|1/2	88.29	37.9	5	C	
FI	Mon	221.5	1.0	3.288	12.94	1.19	1.40	19|10|17	1/2|2|1/2	86.09	41.6	6	C	
FT	Mon	205.9	-4.8	3.422	12.76	1.10	1.33	22|14|16	1/2|2|1/2	55.35	49.7	9	E	7
TW	Mon	212.8	-0.2	7.097	12.57	-	1.63	8|-|8	1|-|1	82.99	35.4	5	E	
TX	Mon	214.1	-0.8	8.702	10.96	1.12	1.33	-|-|-	3|3|5	65.28:	-	5	C	8
TZ	Mon	214.0	1.3	7.428	10.79	1.15	1.34	15|-|15	1|7|1	53.59	41.8	14	C	
VZ	Mon	200.1	1.0	5.091	13.60	1.62:	1.96	46|28|17	1|-|1	32.96	33.6	5	E	9
WW	Mon	202.7	0.3	4.662	12.54	1.22	1.39:	26|19|11	1/4|3|1/2	52.51	51.7	6	E	
XX	Mon	215.5	-1.1	5.456	11.93	1.19	1.42	8|-|8	1|7|1	66.34	43.3	7	C	
YY	Mon	220.1	-2.9	3.455	13.14	1.23	-	-|-|-	3|3|-	-	-	-	-	
V447	Mon	208.1	0.5	2.484	14.11	1.57	1.83:	22|12|17	1/2|2|1/2	55.59	50.8	9	E	
V495	Mon	213.8	-4.5	4.097	12.42	1.33	1.46	18|8|18	1/2|2|1/2	67.44	36.6	8	E	
V508	Mon	208.9	0.9	4.134	10.49	0.91	-	-|-|-	6|7|-	59.35	27.21	23	8	
V510	Mon	210.2	0.3	7.459	12.66	1.53	1.81	13|-|13	1|7|1	63.25	28.47	6	E	9
CR	Ori	195.9	-3.9	4.911	12.30	1.16	1.41	-|-|5	3|3|1	23.62:	35.9	6	C	6
CS	Ori	198.0	-4.5	3.889	11.39	0.95	1.13	-|-|7	3|3|1	38.30	37.2	7	C	
BM	Per	155.7	-0.1	22.952	10.50	1.89	-	21|21|-	4|4|-	-43.86	58.2	16	C/E	
GP	Per	157.9	-3.8	2.042	13.88	1.06	1.34	22|22|8	2|2|2	-51.00:	-	3	E	6
HQ	Per	163.0	-3.3	8.636	11.60	1.23	-	20|20|-	4|4|-	-34.80:	26.8	6	E	
HZ	Per	157.2	-2.5	11.279	13.83:	2.18:	2.58:	24|6|6	4/2|2|2	-29.68	50.3	7	E	
OT	Per	157.2	0.6	26.064	13.55:	2.32:	2.65:	27|27|6	4/2|4/2|2	-44.40	52.4	6	E	
SV	Per	162.6	-1.5	11.129	8.99	1.04	1.24	-|-|-	3|3|5	-5.12	48.8	9	C	
UX	Per	133.6	-3.1	4.566	11.61	1.03	-	-|-|-	3|3|-	-51.83	43.1	12	C	
BC	Pup	238.3	-2.7	3.544	13.88	-	1.61	13|-|13	1|-|1	93.70	41.7	5	E	
CK	Pup	239.8	-4.2	7.418	13.35	-	1.72	13|-|13	1|-|1	125.06	42.9	5	E	
HW	Pup	244.8	0.8	13.453	12.13	1.37	1.54	-|-|-	3|3|5	117.31	42.2	11	C	
VW	Pup	235.4	-0.6	4.285	11.40	1.11	1.32	12|-|12	1|7|1	58.37	40.6	8	C/E	
VZ	Pup	243.4	-3.3	23.164	9.60	1.26	1.38	-|-|-	3|3|5	63.30	-	45	9	
WW	Pup	237.4	1.0	5.517	10.62	0.93	1.09	11|-|10	1|7|1	89.79	45.4	9	C	
WY	Pup	241.8	2.7	5.251	10.61	0.83	0.97	14|-|14	1|7|1	71.73	45.8	8	C	
EZ	Vel	274.9	-1.9	34.535	12.40	1.81	2.07	-|-|-	3|3|5	92.65	50.8	9	C/10	

General data and mean values for the sample cepheids, calculated from the measurements in this paper or collected from the literature. Columns 1-5 indicate the star name, position in galactic coordinates and period. Columns 6-10 give magnitude means for V, B-V, V-I, the number of measurements for each colour resp. (column 9), and the sources (column 10, key below the table.). Columns 11-14 are the γ velocity, the radial velocity amplitude, the number of velocity measurements, the spectrometer used ("C": CORAVEL , "E": ELODIE , number: other source). *Sources*: 1- this paper, 2- Henden (1996, priv. comm.), 3- Berdnikov 1987, 4- Berdnikov 1993, 1995, 5- Caldwell & Coulson 1987, 6- Bersier et al. 1994a, 7- Fernie 1995, 8- Bersier et al. 1994b, 9- Caldwell & Coulson 1985b, 10- Metzger & Schechter 1992. *Key to the notes*: 1- small number of points in photometry, 2- new period from Gessner (1988), 3- not a cepheid according to Antonello et al. 1990, 4- high dispersion in B-V, 5- noisy velocity curve, 6- incomplete phase coverage in radial velocity, 7- new period from Berdnikov, 1993, IBVS 3864, 8- identification uncertain on some velocity points, 9- modified period (this paper)

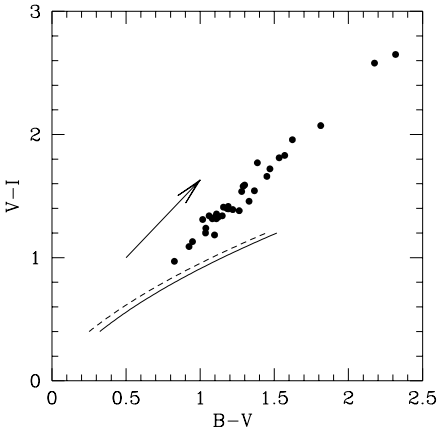

Fig. 4. Colour-colour diagram for the sample: (B-V) vs. (V-I). The points are the measured means, the line the intrinsic locus (Dean et al. 1978). The dotted line is the locus corrected for metallicity effects, using [Fe/H]=-0.5. The arrow is the reddening vector. Bringing the measured colours back on the intrinsic locus using the reddening vector is the "colour-colour" (CC) method of reddening determination. Note that for small periods (small $(B-V)_0$), the angle between the reddening vector and the locus becomes small, and metallicity effects are amplified.

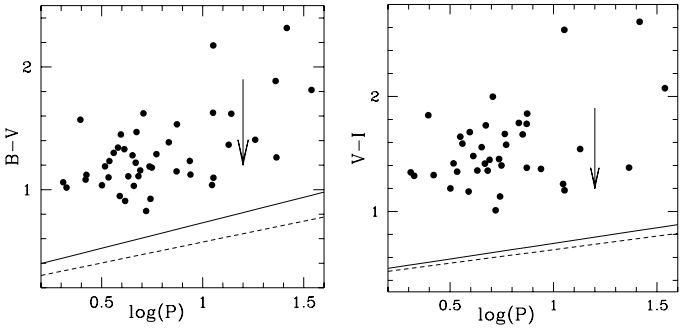

Fig. 5. Period-colour (PC) diagrams for the sample. Left: B-V, right : V-I. The line is the ridge line of the cepheid locus. The dotted line is the relation for [Fe/H]=-0.5. The reddening vector is vertical by definition. Note that the V-I relation is less sensitive to metallicity, and that the uncertainty is not affected by the amount of reddening (see text).

reddenings. We give hereafter two distance determinations with the PC/PL combination, the first with B-V as a colour and V as a magnitude, the second with V-I as a colour and I as a magnitude. We assume throughout that the slopes of the PL and PC relations are unaffected by metallicity (Stothers 1988, Chiosi et al. 1993).

3.1. Distances using (B-V) et V

We used the PC relation from Laney&Stobie (1994), based on 46 galactic cepheids, who find the following corrections for the Magellanic clouds (temperature change + blanketing): $\delta(B-V)_0 = -0.071(LMC)$ and -0.185 (SMC) (45 and 47 objects resp., same source). Assuming $Z_0/Z = 1.4$ and $Z_0/Z = 4$ for the clouds (Feast 1986 and Caldwell & Coulson 1986), we fit the following metallicity corrections on Clouds data:

$$\delta(B-V) = (-0.12 - 0.11 \log P)(1 - Z/Z_0).$$

Then

$$(B-V)_0 = 0.314 + 0.416 \log P + \delta(B-V).$$

We apply the PL relation from the review by Feast & Walker (1987):

$$M_V = -2.78 \log P - 1.35.$$

The bolometric relation is assumed to be independent of metallicity, but the bolometric correction applied to get the PL relation in M_V is metallicity dependent. The correction in Caldwell & Coulson (1987) is used:

$$\Delta B.C. = (0.134(B-V) - 0.046)(1 - Z/Z_0).$$

With (Feast & Walker 1987)

$$R \equiv \frac{A_v}{E(B-V)} = 3.05 + 0.25\,(B-V)_0 + 0.05\,E(B-V)$$

we get the distance modulus:

$$\mu = m_V - M_V - R\,\{(B-V) - (B-V)_0\}.$$

The above relations were calibrated using intensity averages for (B-V), whereas we computed magnitude averages. The first are transformed into the second using Fernie (1990):

$$(B-V)_{int} = (B-V)_{mag} - 0.003 + 0.010\,V_{ampl} - 0.072\,V_{ampl}^2.$$

3.2. Distances using (V-I) and I

Similarly, we use the relations:

$$\delta(V-I) = (-0.027 - 0.053 \log P)(1 - Z/Z_0)$$
$$(V-I)_0 = 0.450 + 0.272 \log P + \delta(V-I)$$

fitted on Magellanic Clouds data from Caldwell & Coulson (1985a).
With the PL relation of Caldwell & Coulson 1987:

$$M_I = -3.45 \log P - 1.39 + \Delta B.C. - \delta(V-I)$$

and (Dean et al. 1978):

$$\eta = 1.250\,(1 + 0.06(B-V)_0 + 0.014E(B-V))$$

one gets

$$\mu = m_I - M_I - \frac{(R-\eta)}{\eta}\,E(V-I).$$

3.3. Choice of distance scale

The second distance determination was preferred when available in the following analysis for the reasons explained in the Appendix, and also because it is less affected by undetected companious (see Sect. 5.3). The Appendix is available electronically at http::://science.springer.

Among the 36 stars with both (V, B-V) and (I, V-I) distances, the dispersion on μ is 0.21 mag, an acceptable value given the intrinsic width of the instability strip, and the mean shift is +0.04 mag (in the sense $\mu_V > \mu_I$)[1].

3.4. Metallicity gradient

Throughout the distance determination, a metallicity gradient of the outer disc of -0.07 dex/kpc is adopted (Harris 1981). The effect of changing this assumption is examined in Sect. 5.3[2].

3.5. Overtone pulsators

The identification of "s-cepheids", characterized by a sinusoidal low-amplitude light-curve, with objects pulsating in the first harmonic mode, has been proposed for some years now (Antonello et al. 1990, Mantegazza & Poretti 1992), and unambiguously confirmed by results from the EROS (Beaulieu et al. 1995) and MACHO (Welch et al. 1995) projects in the LMC.
In our sample, only one star, V510 Mon, was seen to have an abnormally low pulsation amplitude or sinusoidal light curve, though its period of 7 days makes it an unlikely candidate.
The rarity of overtones in the sample could be explained by the decrease in overtone frequency with decreasing metallicity (indicated by SMC data e.g. Buchler & Moskalik, 1994) and a detection bias favoring large amplitudes.

3.6. Type II cepheids

It was realized in 1952 by Baade and others that type II cepheids, though located in the cepheid instability strip, are much smaller, older objects than classical cepheids. It now seems that they do not form a homogeneous population (Harris & Wallerstein 1984).

Distinguishing type II cepheids from classical cepheids is particularly tricky in the outer disc. Kinematically, type II cepheids, nearer but lagging behind young disc rotation, may have the same radial velocity as remoter classical cepheids following young disc rotation. The high z coordinate criterion is not a foolproof discriminant either, since in the outer disc, disc thickening and warping may bring classical cepheids farther from z=0. Finally, a relative number of type II cepheids higher than in the solar neighbourhood may be expected for the outer disc sample since, for a given magnitude, type I cepheids are seen at a larger distance, in remoter places of the outer disc where the stellar density is much lower.

We have applied five criteria to try to detect possible suspects, none of them decisive in isolation:
•high z coordinate. The z coordinates were corrected for the fact that the cepheid plane is lower and slightly tilted relative to the galactic plane (see for instance Fernie 1995). Objects were tagged if farther than 300 pc from the plane $z = 36 + 17d \cdot \sin l$ pc (d is the distance from the sun in kpc).
•low reddening compared to their distance.
•low (P<3 d) or high (P>10 d) period. The distribution of type II cepheids peaks at low ("BL Her" objects) and high ("W Vir" objects) periods compared to classical cepheids.
•position. We tagged stars isolated from any other classical cepheid.
•objects labeled as "CEP" (cepheid of undetermined type) in the GCVS.
Stars with 3 or more of the above criteria were labeled as suspect.

The low velocity dispersion of our sample after the subtraction of differential rotation, about 10 km s^{-1}(see Fig. 10), indicates however that the number of type II cepheids present in the sample is very low (much higher dispersions are expected for type II cepheids, of the order of 30-50 km s^{-1}). The distribution of periods in the sample (Fig. 1) is also typical of classical cepheids and not of type II.

3.7. Position in the Galaxy

Fig. 6 and 7 display the position of the sample cepheids in the Galactic plane and in z, using distances determined here.

4. Galactic rotation

4.1. Axisymmetric solution

With the distances computed in the previous section, and the γ velocities of Sect. 2 (column 1 of Table 1), the rotation curve followed by the sample can be determined.

Assuming a circular rotation around the Galactic Centre, the angular velocity is:

$$\omega = \left(\frac{v_r + v_\odot}{\sin l \cos b} + \theta_0 \right) \frac{1}{R_0}$$

where $v_\odot = u_0 \cos l \cos b + v_0 \sin l \cos b + w_0 \sin b$ is the sun reflex motion.

The rotation velocity is:

$$v_{rot} = R\omega$$

where R is the distance of the object to the Galactic Centre, derived from

$$R = \sqrt{R_0^2 + d^2 \cos^2 b - 2Rd \cos b \cos l}$$
$$d = 10^{\mu/5+1}$$

[1] A campaign to obtain infrared measurements for the southern part of the sample is under way (Pont & Laney, in prep.).

[2] Preliminary calibrations of the metallicity dependence of the surface of the ELODIE cross-correlation function seem to indicate that this value is realistic (Pont et al. 1995).

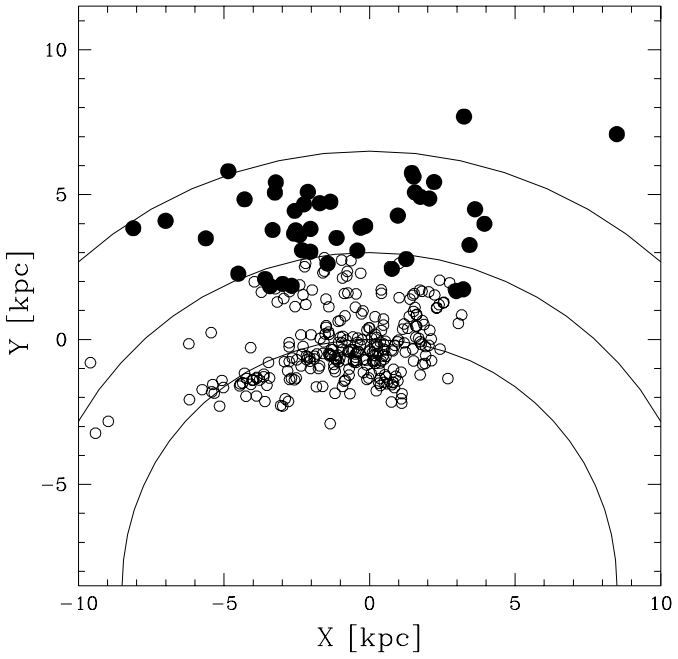

Fig. 6. Position of cepheids in the galactic plane. X and Y are coordinates in kpc. The Sun is at the origin, the Galactic Centre at the bottom. Empty symbols indicate cepheids previously studied for galactic kinematics, solid symbols the cepheids of this sample. Circles are indicated at R=R_0, R=11.5 kpc and R=15 kpc.

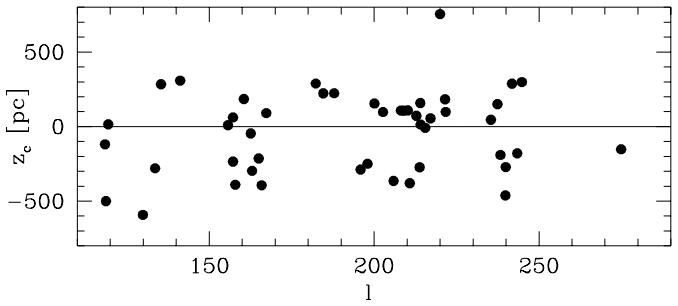

Fig. 7. Position of the cepheids in z relative to the "mean cepheid plane" defined as $z = 36 + 17d \cdot \sin l$ pc, as a function of l. The lack of objects near z=0 is due to the high absorption in the plane.

d is the distance, μ the distance modulus. R_0 (distance of the Sun to the Galactic Centre), θ_0 (rotation velocity of the LSR) and $\boldsymbol{v} = (u_0, v_0, w_0)$ (solar motion relative to the LSR) must be assumed.

We use two sets of (R_0, θ_0):

– (R_0 =8.5 kpc, θ_0 =220 km s^{-1}) recommended in the review by Kerr & Lynden-Bell (1986)

– (R_0 =8 kpc, θ_0 =200 km s^{-1}) indicated by some more recent studies (Merrifield 1992, Pont et al. 1994)

and $\boldsymbol{v}$=(9.3, 11.2, 7.0) km s^{-1} determined from cepheids in Pont et al. (1994).

The resulting rotation and angular velocity curves are displayed in Fig. 8 and 9. The objects labeled as type II suspects are drawn as open circles. Only objects farther than 20^o from the anticentre ($l = 180^o$) are plotted.

Table 2. Constant rotation velocity between 10.5 and 15 kpc fitted to the data, with and without the type II suspects, for two sets of galactic parameters.

R_0 kpc	θ_0 km s^{-1}	V_{rot} all stars km s^{-1}	without suspects km s^{-1}
8.5	220	192.9 ± 3.6	194.5 ± 4.0
8	200	167.2 ± 3.7	169.6 ± 3.9

The sample traces clearly the rotation curve between R=10 and R=15 kpc. It outlines a practically flat rotation curve, slightly below θ_0. Several simple shapes were tried in fitting an analytical rotation curve to the data. A slightly decreasing curve was found. Fitting a linear rotation curve gives:

$$V_{rot} = 192.9 \underset{\pm 3.6}{-} 2.1 \underset{\pm 2.2}{} (R - 12.5) \text{ km s}^{-1}$$

(R_0 = 8.5 kpc, θ_0 = 220 km s^{-1}).

The slope is not significantly different from zero, and $V_{rot} = constant$ was used in the following discussion. Table 2 shows the values of V_{rot} obtained, with or without the type II suspects of Sect 3.6. The fit, of course, is not made in the (R,θ) space, but in the (μ, v_r) space.

The residuals around a flat rotation curve are shown in Fig. 10 (case R_0 = 8 kpc, θ_0 = 200 km s^{-1}). The final dispersion is 10.51 km s^{-1} (9.47 without type II suspects). This value gives an upper limit to the velocity dispersion of cepheids in the outer disc. It is of the order of the local radial dispersion for cepheids, $\sigma_u \simeq 10.4$ km s^{-1} (Pont et al. 1994), and seems to exclude the presence in the sample of a significant number of type II cepheids, since these are expected to have a much larger velocity dispersion, typical of older objects, $\sigma > 30$ km s^{-1}.

4.2. Non-axisymmetric components

A non-axisymmetric component in the rotation of the outer disc can be detected either by a north-south asymmetry in the sample, or, using the control sample near the anticentre, by a radial motion not accounted for by circular rotation.

The fitting of the rotation curve was repeated using only the northern and southern stars separately. The results are V_{rot} = 165.4±6.6 and 169.7±4.7 resp., with no significant difference. Unfortunately, the number of points in the north is not large enough to provide a very strong constraint on the asymmetry.

With the complete sample, including anticentre objects ($160^0 < l < 200^0$, 11 objects), two types of non-axisymmetric components were fitted for:

–a radial motion of the LSR relative to the outer disc (towards the anticentre)

$$v_{rot} = v_{rot}(axisym) + V_{LSR} \cos l \sin b$$

–a uniform expansion of the disc

$$v_{rot} = v_{rot}(axisym) + V_{exp}(R - R_0) \cos \alpha \cos b$$

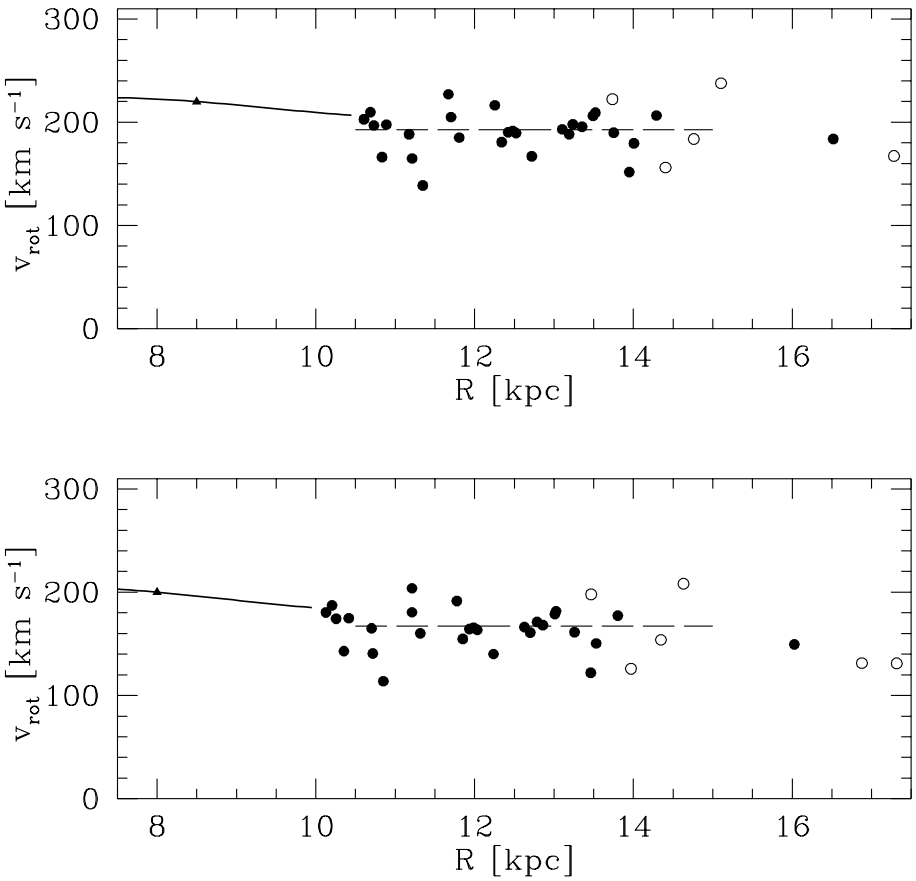

Fig. 8. Rotation curve of the outer disc from cepheids, with R_0 = 8.5 kpc and θ_0 = 220 km s^{-1} (top), or R_0 = 8 kpc and θ_0 = 200 km s^{-1} (bottom). "Type II suspects" (see Sect. 3.6) are plotted as open circles. The rotation curve obtained in Pont et al. (1994) is drawn up to 10.5 kpc. The dashed lines are constant rotation curves at 192.9 km s^{-1} and 167.2 km s^{-1} respectively.

where $\sin\alpha = R_0/R \sin l$.

The results are:

V_{LSR} = +0.46 ± 1.86 km s^{-1}

V_{exp} = −0.39 ± 0.33 km s^{-1}

These values show that non-axisymmetric components are weak or absent. Such radial motions of large amplitude – up to 15 km/s – as have been proposed in some models or suggested by some observations (see for instance Spergel 1993), are not compatible with the cepheid results.

5. Discussion

The determination presented in this paper yields a significantly different value for the rotation velocity compared with previous studies, notably the ones based on HII regions or HI gas (Fich & Tremaine 1991, Merrifield 1992). Fig. 11 compares the HII rotation results reviewed in Fich et al. (1989) with our results. Beyond $R = 1.5R_0$, the first show very scattered data around a rising curve apparently incompatible with the flat or decreasing cepheid rotation curve.

Random or systematic errors on CO and cepheid radial velocities are small and cannot account for the difference. The disagreement can then have two types of causes: either it results from a distance scale difference, or it reveals an intrinsic difference of kinematics between HII regions and cepheids.

5.1. Kinematical difference

A lag on gas rotation of the order of 50 km s^{-1} for objects as young as classical cepheids -generally younger than a galactic orbital period- would be hard to explain. An Inner Lindblad Resonance of the halo could be invoked as a possible cause of the difference in gas and stellar kinematics, an effect mentioned by Spergel (1993). However this model implies an inversion of the radial component of the stellar velocity field around the resonance as well as a sizeable increase in the velocity dispersion, which are not observed (Lewis & Freeman 1989, Blitz & Spergel 1991).

Another cause could be the presence of large radial motions in the gas, induced for instance by spiral arms. Unlike cepheids, HII regions do show a strong north-south asymmetry in their kinematics (see Fig. 11), that could imply large radial motions. If one assumes that the HII regions follow the rotation curve indicated by the cepheids and that the difference is explained by radial motions alone, then the radial motion needed is 20.4 km s^{-1} on average. Although this value is rather large and above what is usually expected from spiral arms, it is not implausible.

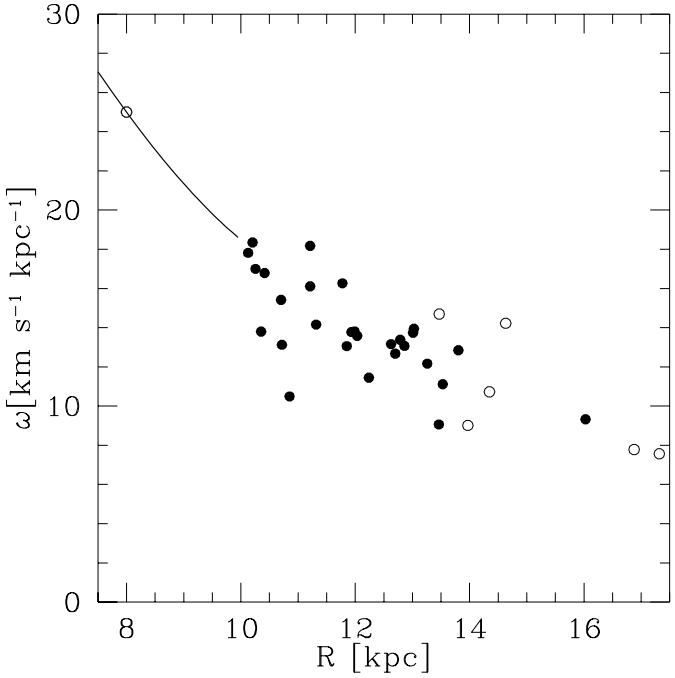

Fig. 9. Angular velocity curve. Symbols as in Fig. 8. R_0 = 8 kpc, θ_0 = 220 km s^{-1} assumed. The advantage of this representation is that the distance errors affects only the horizontal axis.

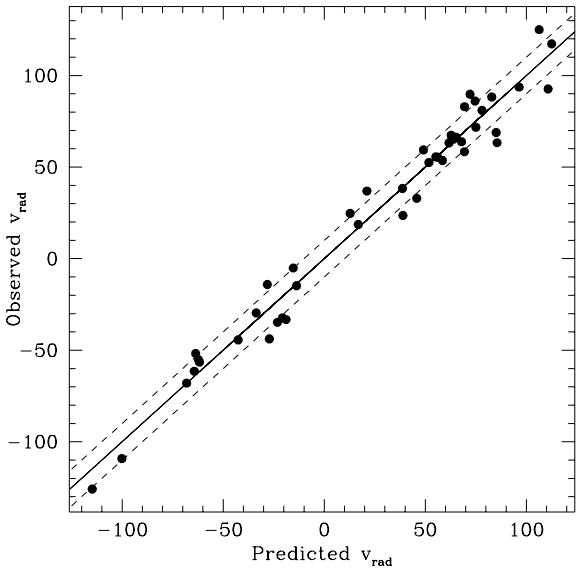

Fig. 10. Observed radial velocities versus velocities predicted from a flat rotation curve with Vrot=192.9 km s^{-1}(R_0 = 8.5 kpc and θ_0 = 220 km s^{-1}). The solid line is $V_{predicted} = V_{observed}$. The two dotted lines indicate $V_{predicted} = V_{observed} \pm 10$ km s^{-1}.

5.2. Distance scale difference

On a rotation curve plot like Fig. 8, an error on distance moves the points *diagonally*, since the distance enters the calculation of both R and V_{rot}. Moreover, an error on the distance modulus μ has an asymmetrical effect on the rotation curve because of the exponential dependence of distance on μ. Therefore a systematic error on μ or a high dispersion on distance determination can artificially cause the rotation curve to appear to be increasing at large R.

The distance shift necessary to bring the HII data of Fich et al. (1989) into agreement with the cepheid data is about 1.2 mag. A distance scale difference of that size is unlikely. On the other hand, the rotation curve of HII regions between R=10 and R=14 kpc has a shape that may awaken some suspicion: its increase is more or less parallel to the line along which a point is moved if its distance is changed while its radial velocity is kept constant. The combination of a distance scale shift and high errors on distances could artificially create such a trend.

We studied this possibility using Monte Carlo simulations: on a synthetic sample orbiting the galactic centre with a constant circular velocity V_{rot} = 200 km s^{-1}, were added a velocity dispersion of 8 km s^{-1}, a dispersion on distances σ_μ, and a systematic distance shift δ_μ. Fig. 12 shows the results of this simulation for three sets of (σ_μ, δ_μ). The conclusion is that it is possible to infer an artificially rising rotation curve similar to the one observed in HII regions, from a tracer with in reality a constant rotation velocity, but with parameters like σ_μ = 0.8 mag and δ_μ = 0.4 mag (Fig. 12 bottom). While high, these values are not unrealistic, given the difficulty of determining HII region distances (Turbide & Moffat 1993). The effect gets even easier to reproduce if the distance scale shift is proportional to R, for instance via metallicity corrections to the theoretical ZAMS.

5.3. Effect of changes in the assumptions

In the previous sections, the cepheid distance scale was considered to be exact. We examine in this section how it is affected by changing some assumptions and by systematic biases. R_0 = 8 kpc and θ_0 = 200 km s^{-1}are assumed. Using (8.5 kpc,220 km s^{-1}) gives very similar results.

PL relation zero-point

The change caused in the derived rotation velocity V_{rot} by a shift in the zero-point of the distance scale ϕ_0 was estimated with Monte Carlo simulations:

$$\Delta V_{rot} \simeq 41 \cdot \Delta\phi_0 \quad \mathrm{km\,s^{-1}}$$

i.e. ΔV_{rot} = 4.1 km s^{-1} for a typical value of 0.1 mag for $\Delta\phi_0$ (Feast & Walker 1987).

Unrecognized type II cepheids

The presence of type II cepheids can bias the results (see Sect. 3.6) because their distance is overestimated by using type I PL relations. If β is the rate of type II in the sample, and θ_{II} their rotation velocity (assumed to be constant), then Monte Carlo simulations indicate:

$$\Delta V_{rot} \simeq \beta(1.20\,\theta_{II} - V_{rot}).$$

θ_{II} is not known. For values of 150 km s^{-1} (thick disc) or 200 km s^{-1} (old disc, as proposed by Harris & Wallerstein

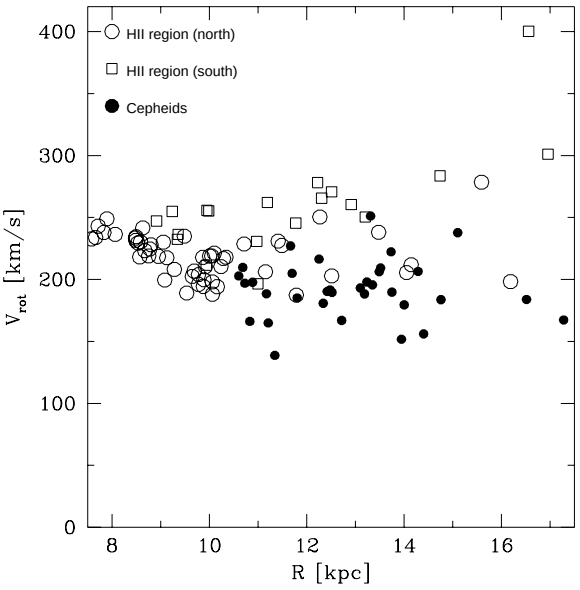

Fig. 11. Comparison of HII region and cepheid rotation curve data. Open circles: HII regions (north), open squares: HII regions (south), filled circles: cepheids. The increase at large radii towards $V_{rot} \sim 250\,\mathrm{km\,s^{-1}}$ is not observed in the cepheids.

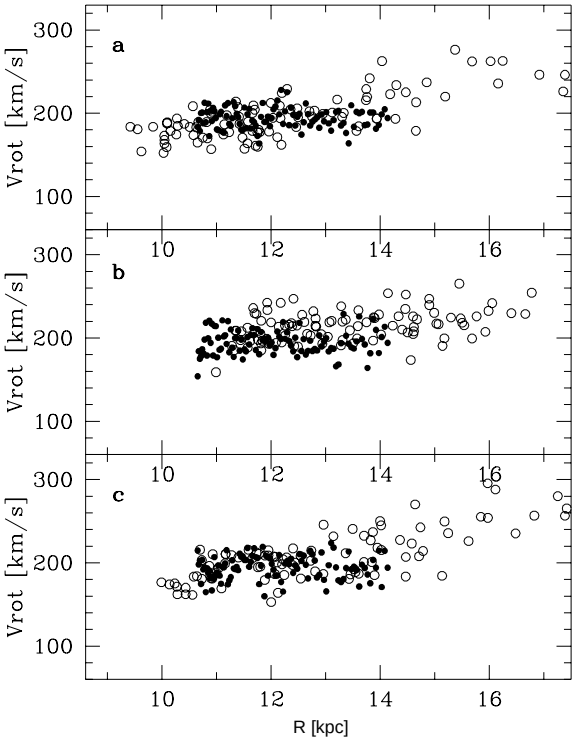

Fig. 12. Monte Carlo simulations showing the effect of distance uncertainties on the rotation curve. The filled circles show the "true" synthetic data, with $\sigma_{v_r} = 8\,\mathrm{km\,s^{-1}}$, and the open circles the data recovered after adding a distance dispersion σ_μ and a systematic shift δ_μ. The results are displayed for three sets of parameters (σ_μ, δ_μ): 1.0 mag, 0 (a); 0.2 mag, 0.6 mag (b); 0.4 mag, 0.8 mag (c). The plot (c) shows how a rotation curve similar to the one observed in HII regions can result from a lower, flat rotation curve once distance dispersion and shift are added.

1984), one gets, with β=0.1, ΔV_{rot} = –1.4 and +4.6 $\mathrm{km\,s^{-1}}$ respectively.

Binaries

The presence of an unrecognized companion causes the distance of a cepheid to be miscalculated. The radial velocities are also affected, but in a non-systematic way, only amounting to an increase in the final dispersion. In none of the sample objects was a change in the γ velocity detected.

The effect of undetected binaries was simulated by adding synthetic blue main-sequence companions inspired from Evans (1992, 1995). We assumed a companion rate of 20%, with a frequency proportional to ΔM_{bol}, to a maximum of ΔM_{bol} = 4 mag, and then computed the effect on the inferred reddenings and distances.

Distances from PC(B-V) and PL(V) (Sect. 3.1) can be affected. The net effect is $\Delta V_{rot} \simeq 4\,\mathrm{km\,s^{-1}}$. Distances from PC(V-I) and PL(I) are much less sensitive, with $\Delta V_{rot} \simeq 0.5\,\mathrm{km\,s^{-1}}$.

Metallicity corrections

Repeating the entire procedure with different values for the assumed metallicity gradient in the disc ($G \equiv \partial[Fe/H]/\partial R$) gives the following relations:

ΔV_{rot} = +56 ΔG km s^{-1} (V-I, I distances)
ΔV_{rot} = +176 ΔG km s^{-1} (B-V, V distances)

e.g. changing the gradient from -0.07 dex kpc^{-1} to -0.03 dex kpc^{-1} increases V_{rot} by 2.2/7.0 km s^{-1}.

Position in the instability strip

The photographic detection of faint cepheids near the magnitude limit favours objects on the blue and bright side of the instability strip, a bias pointed out by Feast (1995). In terms of the notation used in the appendix, it means $<\Delta M_V><0$ in Eqs. (3) and (4). We modeled this bias and found that with a width of the instability strip of 0.6 mag in V, it causes an overestimation of distances by 0.03 mag in (V-I,M_I) and 0.08 mag on average in (B-V,M_V) (or 1-2 km s^{-1}on V_{rot}) if the cepheid detection limit can be modelled as a simple magnitude cutoff. As the second distances are in our sample already larger on average than the first, it is likely that the bias is not significant.

5.4. Non-axisymmetric models of the Galaxy

The cepheid data can be compared with some recent suggestions for non-axisymmetric models of the Galaxy. The model by Kuijken (1994), assuming an m=1 asymmetry, implies a radial motion of the LSR. Blitz & Spergel (1991) propose in their

elliptical model a radial motion of the LSR of 14 km s^{-1} relative to the outer disc, to explain features observed in gas kinematics. The value obtained here, 0.46 ± 1.86 km s^{-1}(Sect. 4.2), is not compatible with this model. It can be compared with other observational results, such as Lewis & Freeman (1989) or Metzger & Schechter (1994), that give significant LSR motions in the opposite direction. The fact that the cepheids show an LSR radial motion intermediate between younger and older objects could indicate an age dependence of radial motion in the outer disc.

In fact, there is no strong evidence in the cepheids for any non-axisymmetric component in the rotation. However, as pointed out by Kuijken (1993), the outer disc velocity field is sensitive to any non-axisymmetric component, but is not a good detector of it.

6. Conclusion

Outer disc cepheids indicate a flat or slightly decreasing rotation curve between R=10 and R=15 kpc, corresponding to V_{rot} = 193 km s^{-1}for (R_0 = 8.5 kpc, θ_0 = 220 km/s) or V_{rot} = 167 km s^{-1}for (R_0 = 8 kpc, θ_0 = 200 km/s), with an internal error of about 4 km s^{-1}and possible systematic effects amounting to approximately 6 km s^{-1}when summed quadratically. The problem of the increase at large radii, as seen for instance in the curve by Clemens (1985), that was difficult to understand dynamically and uncharacteristic of galaxies such as the Milky Way, seems to vanish.

The mismatch between the cepheid and HII region rotation curves may indicate either important non-axisymmetric motions in the gas that are smoothed out in the stellar velocity field, or high uncertainties and zero-point shift on the distances of HII regions. These two possibilities can be studied more closely in the future. In the first case, a gradual change from gas kinematics to stellar kinematics would be predicted in the cepheids as a function of their age, ranging from a few Myr to some 10^2 Myr, as they move from gas to stellar kinematics. This could be observed with a sufficient number of outer disc cepheids. In the second case, new metallicity-dependent models, combined with CCD observations, could yield a more secure HII region distance scale.

In both cases, the cepheid rotation curve is a better indicator of the rotation of the stellar disc, and should be used for kinematical distance determinations. The outer disc velocity field derived from HII regions (see Brandt & Blitz 1993), including non-axisymmetric motions, is thus probably not an accurate indicator of the *stellar* velocity field.

No evidence for significant non-axisymmetric motions is found in our data. It is possible that either the triaxiality of the Galaxy is not as important as predicted by some models, or that the outer disc cepheids are locally not greatly affected.

Increasing the number of outer disc cepheids studied would obviously be desirable, in order to provide tighter constraints on the north-south asymmetry, the radial motion, and the rotation curve for R=15-16 kpc. Most known classical cepheids in the outer disc have been included in the sample. Completeness arguments alone indicate that a large number remain to be discovered. However the absorption in the plane of the disc, combined with the decreasing density, would make a search for new remote cepheids very ineffective in the visible. The infrared should be more promising, although the effort implied is still considerable. The area to be scanned covers several hundreds of square degrees, and the harvest may not be plentiful. Large infrared surveys such as DENIS may contribute to this effort.

ELODIE spectra obtained for this study can also be used to determine metallicities using cross-correlation techniques. This gives in-situ metallicities in the outer disc. We are now calibrating this method (Pont et al. 1995). A study of cepheid colours, combined with infrared observations, is also under way (Pont&Laney, in prep.), to study with more accuracy the effect of metallicity on intrinsic colours.

Acknowledgements. It is a real pleasure to thank Arne Henden for providing us with abundant photometric data on the northern part of the sample. We are also indebted to the people who helped with the CORAVEL observations. Discussions with Dave Laney and John Caldwell have been enlightening with respect to the distance problem. S. Udry, R. Fux and A. McFarlaine have been kind enough to proof-read the paper and make comments. We thank the anonymous referee for his extremely careful reading of the manuscript. This work was supported by the Swiss National Science Foundation and the University of Geneva. It has made use of the SIMBAD database operated at CDS, Strasbourg, France, and the McMaster Cepheid Archive.

References

Antonello E., Poretti E., Reduzzi L., 1990, A&A 236, 138
Baranne A., Mayor M., Poncet J.L., 1979, Vistas in Astronomy 23, 279
Baranne A., Queloz D., Mayor M. et al., 1996, A&A , in press
Beaulieu J.-P., Grison P., Tobin W. et al, 1995, A&A , in press
Berdnikov L.N., 1987, Perem. Zv. 22, 505
Berdnikov L.N., 1993, Pisma A.Zh. 19, 210
Berdnikov L.N., 1995, Pisma A.Zh. 21, 340
Bersier D., Burki G., Burnet M., 1994a, A&AS 108, 9
Bersier D., Burki G., Mayor M. et al., 1994b, A&AS 108, 25
Blecha A., Weber L., Simond G. et al., 1990, in A.S.P. Conf.Ser. 8, Ed. G.H. Jacoby, p. 192
Blitz L., Spergel D., 1991, ApJ 370, 205
Brandt J., Blitz L., 1993, ApJ 275, 67
Bratschi P., Blecha A., 1996, in preparation
Buchler J.R., Moskalik P., 1994 A&A 292, 450
Caldwell J.A.R., Coulson I.M., 1985a, MNRAS 212, 879
Caldwell J.A.R., Coulson I.M., 1985b, South Afr. Obs. Circ. 9, 5
Caldwell J.A.R., Coulson I.M., 1986, MNRAS 218, 223
Caldwell J.A.R., Coulson I.M., 1987, AJ 93, 1090
Chiosi C., Wood P.R., Capitanio N., 1993, ApJS 86, 541
Clemens D.P., 1985, ApJ 295, 422
Cousins A.W.J., 1974, MNASSA 33, 149
Dean J.F., Warren P.R., Cousins A.W.J., 1978, MNRAS 183, 569
Dwek E., Arendt R.G., Hauser M.G. et al., 1995, ApJ 445, 716
Evans N.R., 1992, ApJ 382, 220
Evans N.R., 1995, ApJ 445, 393
Feast M.W., 1986, in IAU Symp. 108, ed. S. van den Bergh, p.157

Feast M.W., 1991, in Observational Tests of Cosmological Inflation, ed. T. Shanks et al., Kluwer, p.147
Feast M.W., 1995, in ASP Conf. Ser. 83., eds. Stobie R.S. and Whitelock P.A., p. 209
Feast M.W., Walker A.R., 1987, ARA&A 25, 345
Fernie J.D., 1990, ApJ 354, 295
Fernie J.D., 1995, in ASP Conf. Ser. 83., eds. Stobie R.S. and Whitelock P.A., p. 155
Fernie J.D., Beattie B., Evans N.R. et al., 1995, IBVS No 4148
Fich M., Blitz L., Stark A.A., 1989, ApJ 342, 272
Fich M., Tremaine S., 1991, ARA&A 29, 409
Freedman W.L., Madore B.F., 1990, ApJ 365, 186
Gessner H., 1988, Mitt. über Ver. St. 11 H. 7, 84
Harris H.C., 1981, AJ 86, 707
Harris H.C., Wallerstein G., 1984, AJ 89, 379
Henden A., 1996, preprint
Hron J., 1987, A&A 176, 34
Joy A.H., 1939, ApJ 89, 356
Kerr F.J., Lynden-Bell D. 1986, MNRAS 221, 1023
Kholopov P.N., 1985, General Catalogue of Variable Stars, ed. Nauka, Moskow
Kuijken K., 1993, in "Back to the Galaxy", AIP Conf. Proc. 278., ed. S. Holt and F. Verter, p. 560
Kuijken K., 1994, PASP 104, 809
Kuijken K., Tremaine S., 1994, ApJ 421, 178
Laney D., Stobie B., 1994, MNRAS 266, 441
Lewis J., Freeman K.C., 1989, AJ 97, 139
Mantegazza L., Poretti E., 1992, A&A 261, 137
Manfroid J., 1985, PhD thesis, Univ. of Liége
Menzies J.W., Marang F., Laing J.D. et al., 1991, MNRAS 248 642
Merrifield M.R., 1992, AJ 103, 1552
Metzger M.R., Caldwell J.A.R., Schechter P.L., 1992, AJ 103, 529
Pont F., Mayor M., Burki G., 1994, A&A , 285, 415
Pont F., Queloz D., Bratschi P. et al., 1995, in ASP Conf. Ser. 83., eds. Stobie R.S. and Whitelock P.A., p. 194
Rufener F., 1988, A&AS 78, 469
Rufener F., Nicolet B., 1988, A&A 206, 357
Schneider S.E., Terzian Y., 1983, ApJ 274, L61
Spergel D., 1993, in "Back to the Galaxy", AIP Conf. Proc. 278. ed. S. Holt and F. Verter, p. 337
Stibbs D.W.N., 1956, MNRAS 116, 453
Stift M.J., 1995, A&A 301, 776
Stothers R.B., 1988, ApJ 329, 712
Thuan T.X., Gunn J.E., 1976, PASP 88, 543
Turbide L.,Moffat A., 1993, AJ 105, 1831
Wachmann, A. A., 1966, Abh. Hamb. Sternw. VII No 7, 341
Weinberg M.D., 1992, ApJ 384, 81
Welch D.L., Alcock C., Bennett D.P. et al. 1995, in ASP Conf. Ser. 83., eds. Stobie R.S. and Whitelock P.A., p. 232

This article was processed by the author using Springer-Verlag LaTeX A&A style file *L-AA* version 3.